OH kinetics and photochemistry of HNO 3 in the presence of water vapor

ARTICLE *in* CHEMICAL PHYSICS LETTERS · JUNE 2001

Impact Factor: 1.9 · DOI: 10.1016/S0009-2614(01)00468-7

4 AUTHORS, INCLUDING:

Geert K. Moortgat
Max Planck Institute for Chemistry
261 PUBLICATIONS **9,030** CITATIONS

15 June 2001

ELSEVIER

Chemical Physics Letters 341 (2001) 93–98

CHEMICAL PHYSICS LETTERS

www.elsevier.nl/locate/cplett

OH kinetics and photochemistry of HNO_3 in the presence of water vapor

Shaun A. Carl [a,1], Trevor Ingham [a,2], Geert K. Moortgat [a], John N. Crowley [a,*]

[a] *Max-Planck-Institut für Chemie, Division of Atmospheric Chemistry, Postfach 3060, 55020 Mainz, Germany*

Received 15 March 2001; in final form 9 April 2001

Abstract

The pulsed-laser-photolysis technique was used to determine the rate constant of the gas-phase reaction between the hydroxyl radical (OH) and HNO_3 for the first time under conditions of high relative humidity at (295 ± 3) K. The value obtained, at a total pressure of 200 Torr N_2, was $1.64^{+0.11}_{-0.20} \times 10^{-13}$ cm^3 s^{-1} (error limits include assessment of systematic errors), in excellent agreement with the most recent determinations [J. Phys. Chem. 103 (1999) 3031], and was invariant with relative humidity up to 0.50. The shape of the HNO_3 absorption bands between 210 and 350 nm also showed negligible variation with relative humidity.

1. Introduction

Nitrogen oxides play an extremely important role in tropospheric photochemistry, where they participate in catalytic cycles involving the oxidation of CH_4, non-methane hydrocarbons, and CO, that can lead either to overall production or to overall loss of $[O_3]$ and $[HO_x]$.

$$NO + O_3(\text{or } RO_2) \rightarrow NO_2 + O_2(\text{or } RO), \quad (1)$$

$$NO_2 + h\nu(+O_2) \rightarrow NO + O_3, \quad (2)$$

where R represents H or an organic group (e.g. $CH_3, CH_3C(O)$). HNO_3 is a major oxidation product of NO_x and acts as a relatively stable reservoir for active nitrogen:

$$NO_2 + OH + M \rightarrow HNO_3 + M, \quad (3)$$

$$HNO_3 + h\nu \rightarrow NO_2 + OH, \quad (4)$$

$$HNO_3 + OH \rightarrow NO_3 + H_2O. \quad (5)$$

Reactions (1) and (2) establish the fast photochemical equilibrium between NO and NO_2, whereas reactions (3)–(5) set up the HNO_3–NO_x photochemical cycle, which can reach steady state in 1–3 days, depending on altitude. To a first approximation, the magnitude of the HNO_3/NO_2 ratio depends on the relative rates of activation and de-activation of NO_x in the above gas-phase processes, though the heterogeneous hydrolysis of N_2O_5 to HNO_3 can also play a role in some parts of the troposphere [2]. Presently there is a discrepancy between field measurements and the

* Corresponding author. Fax: +49-6131-305436.
E-mail address: crowley@mpch-mainz.mpg.de (J.N. Crowley).
[1] Present address: Department of Chemistry, University of Leuven, Celestijnenlaan 200 F, 3001 Heverlee, Belgium.
[2] Present address: Jet Propulsion Laboratory, California Institute of Technology, Mail Stop 183-901, 4800 Oak Grove Drive, Pasadena, CA 91109, USA.

0009-2614/01/$ - see front matter
PII: S0009-2614(01)00468-7

predictions of photochemical models of the $[HNO_3]/[NO_x]$ ratio in the remote, free troposphere, in which models persistently predict this ratio to be significantly larger than has been measured (see e.g. [2,3] and references therein) though some of this discrepancy may be resolved by using updated rate coefficients for some key reactions of NO_2 and HNO_3 [4]. In this work we present results of experimental investigations into the possibility that the chemical reactivity of HNO_3 towards the OH radical (5) is modified by the presence of water vapor. Rationale for this hypothesis is provided by drawing analogy to the HO_2 self-reaction (6), which, like the reaction of OH with HNO_3, is bimolecular, yet has a pronounced pressure dependence. The pressure dependence of reaction (5) has been rationalized in terms of formation of a vibrationally excited association complex, $OH–HNO_3^*$, which may either dissociate back to reactants or be stabilized by collision and proceed to products. The HO_2 self-reaction is also believed to owe its pressure dependence to initial formation of a vibrationally excited HO_2–HO_2 association complex. In addition, the rate constant for reaction (6) is known to be significantly influenced by the presence of water vapor, with the rate constant enhanced by a factor 1.7 at 10 Torr of H_2O and 298 K [5] compared to dry conditions. In the lower troposphere, and especially in tropical regions, H_2O concentrations in excess of 10 Torr are often encountered (1 Torr = 133 Pa).

$$HO_2 + HO_2(+H_2O) \rightarrow H_2O_2 + O_2(+H_2O). \quad (6)$$

To date, all experimental data (see [4] for a summary) obtained on the reaction of OH with HNO_3 have been obtained in the absence of H_2O vapor or under conditions of very low relative humidity. If a similar dependence on H_2O vapor exists as seen for the HO_2 self-reaction, these data may not be applicable to all of the atmosphere. In the present work, we examine the possibility that the presence of H_2O can enhance the rate constant of reaction (5), either by more efficiently quenching the association complex, or by forming a complex with HNO_3 in the gas-phase, that increases the rate of stabilization of the modified (larger) association complex.

Apart from reaction with OH, the regeneration of NO_x from HNO_3 also occurs via photodissociation, the rate of which depends on the magnitude of overlap with solar actinic flux (i.e., on the UV absorption spectrum of HNO_3) and on the quantum yield for dissociation. The UV absorption spectrum and photodissociation quantum yields of HNO_3 may potentially be modified in the presence of H_2O if strong molecular interactions can alter the geometry of either its ground state or the dissociating excited states. A change in the absorption cross-section of HNO_3 would have greatest impact at wavelengths greater than 290 nm where the tropospheric actinic flux rises sharply. For this reason, we have re-measured the absorption cross-sections of HNO_3 in dry bath gas, and in the presence of up to 8 Torr of H_2O between 210 and 350 nm.

2. Experimental

The experimental apparatus has been described in detail elsewhere [6]. For the present experiments, a Pyrex cylinder, 6.5 cm in diameter, with a heated quartz window attachment ($\approx$30 K above ambient) at each end, was used as the reaction vessel. The quartz windows provided coupling for three optical beams, from an excimer laser, a deuterium lamp and a diode laser to the gaseous mixture for purposes of generation of OH (reaction (4)), and for monitoring reactant and product concentrations. All three beams traveled along the cylindrical axis of the reaction vessel, each beam having a total path length of 104 cm.

HNO_3, diluted to ca. 1% in N_2 (99.999% purity), or Ar (99.999% purity) for some measurements, was introduced to the reaction vessel from a blackened 10 L bulb. N_2 was admitted into the vessel directly from its cylinder via a flow controller to achieve the desired total pressure of 200 Torr at (295 ± 3) K. The reaction vessel was then isolated from the mixing lines and pumps, and the optical/kinetic measurements were carried out on the static gas mixture.

Reaction (5) was initiated by generating OH radicals through photo-dissociation of a small fraction of HNO_3 (typically 5×10^{-4}) using a

pulsed excimer laser (25 ns pulse duration) operating at 248 nm. The apertured photolysis beam of diameter 7 mm traveled through a relatively small volume of the HNO_3/N_2 or $HNO_3/N_2/H_2O$ mixture along the vessel's cylindrical axis and well away from its wall. The course of reaction (5) was followed for several milliseconds after the photolysis pulse by continuously monitoring the resulting product, NO_3, via its absorption band centered at 662 nm ($\sigma_{662\ nm} = 2.1 \times 10^{-17}$ cm^2 [7]), using a 3 mW, cw diode laser operating at $\lambda = 662.1$ nm. The diode laser beam traveled along the same path as the photolysis beam and within the volume swept out by it, before its relative intensity was measured using a photomultiplier tube (PMT). The stability of the diode laser beam intensity on the millisecond time scale allowed a NO_3 concentration profile with a good signal-to-noise ratio to be constructed by averaging 10 absorption profiles at 0.2 Hz.

The concentration of HNO_3 was determined by monitoring the attenuation of light from a D_2 lamp between 210 and 290 nm using an intensified, diode array detector and comparison with the current recommendation of cross-sections for HNO_3 at 295 K [5]. By this method, HNO_3 concentrations, which are needed for the determination of the rate constant, are known to ±5%. In a separate set of experiments, the optical absorption of HNO_3 was measured both in the presence and absence of H_2O between 290 and 335 nm: the wavelength region responsible for most of HNO_3 photolysis in the troposphere. These measurements were similar to those carried out for monitoring HNO_3 concentrations in the reaction cell, the main differences being use of a 174 cm long absorption cell equipped with monochromator, diode array and deuterium lamp. Spectra were collected for mixtures of HNO_3 vapor in N_2, and of HNO_3 vapor and H_2O (8 Torr) in N_2 to a total cell pressure of 100 Torr. Both HNO_3 vapor and H_2O were admitted to the absorption cell directly from their liquid reservoirs. Pure HNO_3 (liq) was prepared by reaction of H_2SO_4(liq) (99% purity) with KNO_3(s) (greater than 99% purity) under vacuum at 273 K. Optical measurements on the HNO_3(g) revealed an initial impurity of NO_2 of less than 0.5%.

3. Results

3.1. Kinetic measurements

The determination of the rate constant of reaction (5), utilizes NO_3 as a spectroscopic marker for OH. Formation of NO_3 and H_2O, as written in reaction (5), is the only significant reaction pathway [8]. In the absence of any other loss processes for NO_3 and OH, the time profile of NO_3 following the Excimer pulse may then be expressed as

$$[NO_3]_t = [OH]_0\{1 - \exp(-k_5' t)\}, \quad \text{(i)}$$

where $k_5' t = k_5[HNO_3]$. In the presence of other removal processes for both NO_3 and OH, which is mainly provided by the NO_2 impurity in the HNO_3 sample, the time dependence of $[NO_3]$ takes the following form:

$$[NO_3]_t = [OH]_0 A \exp(-k_7' t) - \exp(-(k_5' + k_3')t), \quad \text{(ii)}$$

where $A = k_5'/(k_5' + k_3' - k_7')$, $k_3' = k_3[NO_2]$ and $k_7' = k_7[NO_2]$, and k_3 and k_7 are the bimolecular rate constants for reactions (7) and (3) at the pressure and temperature of the measurements, respectively.

$$NO_2 + NO_3 + M \rightarrow N_2O_5 + M. \quad (7)$$

Diffusion of OH or NO_3 out of the observation region was negligible on the time scales of collection of a NO_3 decay.

k_5' was derived by computer fitting the $[NO_3]_t$ profiles to Eq. (ii), using literature values of k_3 and k_7 at the appropriate pressure and temperature, and allowing both $[OH]_0$ and $[NO_2]$ to vary. Note that the result obtained does not depend on absolute values of k_3 and k_7, but on their relative value (see below). The loss rate of OH due to reaction with NO_2 was always less that 15% of its loss rate due to reaction with HNO_3.

Fig. 1 shows examples of NO_3 concentration profiles derived from absorption measurements at 662 nm following 248 nm photolysis of HNO_3 in the presence of 10 Torr H_2O vapor. Each $[NO_3]$ profile is related to a different HNO_3 concentration. The time dependence of the NO_3 profiles are well described by Eq. (ii) (solid lines). A numerical simulation [9] of the chemical system using

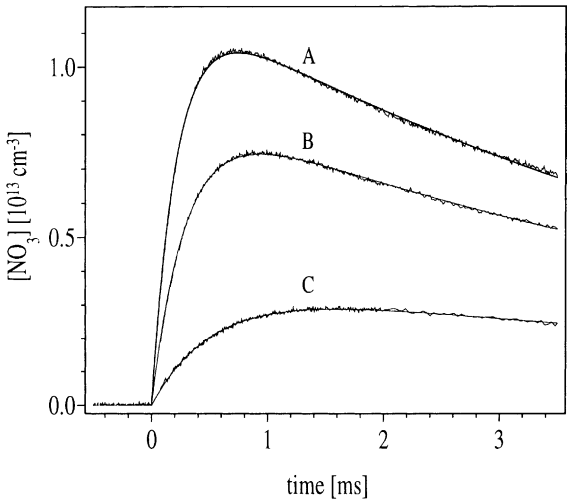

Fig. 1. Examples of $[NO_3]$ derived from absorption measurements at 662 nm following pulsed photolysis of HNO_3 vapor at 248 nm in the presence of 10 Torr of H_2O vapor. (a) $[HNO_3] = 2.28 \times 10^{16}$ cm^{-3}; (b) $[HNO_3] = 1.66 \times 10^{16}$ cm^{-3}; (c) $[HNO_3] = 9.07 \times 10^{15}$ cm^{-3}. Solid lines are best fits to Eq. (ii).

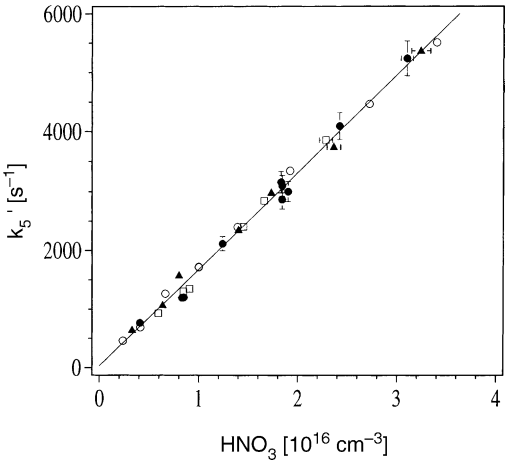

Fig. 2. Plot of k_5' versus HNO_3 concentration. Solid triangles, $p(H_2O) = 3$ Torr; solid circles, $p(H_2O) = 6$ Torr; open squares, $p(H_2O) = 10$ Torr; open circles, $p(H_2O) = 0$ Torr.

recommended rate constants [4,5] showed that at the laser fluences used the reaction of OH with NO_3 ($k = 2.2 \times 10^{-11}$ cm^3 s^{-1}) does not substantially influence the NO_3 profile, and an error (overestimation) in the rate constant arising because of this reaction would be $\leqslant$10%. In addition, the OH self-reaction (to form H_2O_2) accounted for no more than 1% of its overall loss rate.

Fig. 2 summarizes the pseudo first-order rate constants derived from the $[NO_3]$ profiles (k_5') as a function of HNO_3 concentration in the presence of 3, 6 and 10 Torr of water vapor and in dry N_2 bath gas, all at a total pressure of 200 Torr. An examination of this figure shows that is there is no significant difference between the data sets obtained at different humidity. For this reason we quote a value of k_5 obtained from all the data of: $1.64^{+0.11}_{-0.20} \times 10^{-13}$ cm^3 s^{-1}, independent of the concentration of H_2O between 0 and 10 Torr. The error limits are derived from an assessment of systematic errors, and include the effect of varying the k_3/k_7 ratio by $\pm$30%, an uncertainty of 5% for the HNO_3 concentration and the effects of secondary removal of OH and NO_3 via their reaction (see text above) which can result in an overestimation of k_5 by max 10%.

The 295 K, 200 Torr rate constant thus derived is in excellent agreement with the currently recommended value [4] for this reaction at 295 K and 200 Torr of N_2 of 1.56×10^{-13} cm^3 s^{-1}.

3.2. Absorption spectrum of HNO_3

Absorption due to HNO_3 both under 'dry' conditions and under conditions of high relative humidity was recorded in the wavelength region 210–286 nm in order to derive HNO_3 concentrations needed for the kinetic analysis (see above). Similar spectroscopic measurements were carried out with water pressures of 3 and 6 Torr, and in the absence of water vapor. In all cases, the variation of optical density with wavelength showed the same functional form. This indicates the reliability of this method to monitor $[HNO_3]$ in the presence of large concentrations of H_2O, and further shows that there are no changes in shape of the HNO_3 absorption spectrum ($\pm$2%) due to the presence of H_2O in this region of the spectrum.

This region of the spectrum is however not important for the photodissociation of HNO_3 in the lower atmosphere where it occurs predominantly between 290 and 335 nm. The photolysis rate of HNO_3 falls off at the shorter wavelength

side of this range due to a rapidly decreasing actinic flux, and becomes negligible at $\lambda < 290$ nm. The long wavelength fall-off of photolysis rate is due to the decreasing absorption cross-section of HNO_3, and photolysis again becomes negligible at $\lambda > 335$ nm. For this reason we made a detailed study of the influence of H_2O vapor on the absorption spectrum of HNO_3 between 290 and 350 nm.

Fig. 3 shows an absorption profile obtained in the presence of 10 Torr water vapor. The uppermost curve is raw data before numerically stripping the absorption due to the NO_2 impurity (dashed line) in the HNO_3 sample. A small amount of structure remains in the resultant absorption (monotonically decreasing with wavelength) at $\lambda > 330$ nm due to signal noise and to a very small, miscancelled NO_2 residual absorption. The signal-to-noise ratio becomes unity at about 340 nm. The absorption spectrum is, however, plotted to 350 nm, and compared with the recommended literature spectrum of HNO_3 at 5 nm intervals (circles). Clearly there is good agreement, and no significant deviation due to the presence of H_2O is observed.

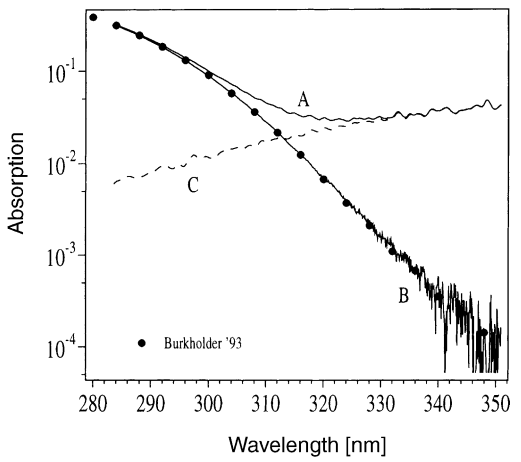

Fig. 3. The absorption spectrum of HNO_3 between 290 and 350 nm measured in the presence of 8 Torr of H_2O vapor under 0.4 nm resolution. Curve (A) shows the raw spectra containing contributions due to the absorption of NO_2. Curve (B) shows the remaining absorption spectrum due to HNO_3 following numerical stripping of the NO_2 absorption (curve C). Burkholder '93, Relative absorption based on the literature recommendation for the HNO_3 spectrum [14].

By plotting the ratio of HNO_3 absorption obtained both under wet and dry conditions in this study (not shown), we can put an upper limit of 15% to an enhancement of the HNO_3 absorption cross-sections at $\lambda > 320$ nm. Although this might at first glance seem significant, we note that at wavelengths greater than 315 nm the contribution to HNO_3 photolysis rapidly falls, thus the total J-value for dry HNO_3 compared to 'wet' HNO_3 are unlikely to be significantly different. Calculations of HNO_3 J-values for ground level, 50°N, solar zenith angle 25° and a column density of 300 DU using both wet and dry spectra results in values that agree within ±1% even if the upper limit of 15% is used.

4. Discussion

Our results have shown that neither the kinetics of the reaction of OH with HNO_3 nor the absorption cross-section of HNO_3 are influenced by water vapor. We now consider why this is the case, and where the differences between the HO_2 self-reaction (which is strongly influenced by the presence of H_2O) and the reaction of OH with HNO_3 lie. It is believed [10,11] that the enhancement in rate constant for the HO_2 self-reaction in the presence of water vapor is due to the efficient formation of a complex between HO_2 and H_2O:

$$HO_2 + H_2O + M \Longleftrightarrow HO_2 \cdot H_2O + M, \qquad (8)$$

which is now known to be formed with a binding energy of ≈30 kJ/mol [12]. The significant increase in the vibrational degrees of freedom of the $HO_2 \cdot H_2O$ complex compared to the free HO_2 radical can account for the increase in the rate constant of the HO_2 self-reaction if a significant fraction of HO_2 (and thus the association complex formed) is bound to $H_2O \cdot HNO_3$ can also form a complex with a water molecule:

$$HNO_3 + H_2O + M \Longleftrightarrow HNO_3 \cdot H_2O + M \qquad (9)$$

and indeed the binding energy (≈40 kJ/mol [13]) is even greater than that of HO_2. The important difference between the H_2O complexes of HO_2 and HNO_3 is related to the equilibrium fraction of complex compared to free molecules. In the case of

HO_2, the equilibrium fraction of $HO_2 \cdot H_2O$ at 298 and 100% humidity ($\approx$10 Torr H_2O) is calculated to be >50% [12]. For HNO_3, despite the larger binding energy of the complex compared to HO_2, an unfavorable change in entropy means that the fraction of complexed HNO_3 under the same conditions is estimated to be only 1% [13]. Thus, even if a $HNO_3 \cdot H_2O$ complex were to react five times as rapidly with OH as free monomeric HNO_3, at such low equilibrium concentrations, no detectable change in rate constant in our experiments, nor a significant enhancement in the rate of this process in the atmosphere is to be expected. The equilibrium constant for $HNO_3 \cdot H_2O$ formation is strongly temperature dependent, and complex formation is favored at low temperatures such as those found around the tropopause. We note also that the pressure dependence of the reaction between OH and HNO_3 is greater at low temperatures [1] and thus would expect that any third-body effect of H_2O would be maximized under these conditions. However, these positive effects which may be expected at low temperatures are more than offset by the reduction in the equilibrium vapor pressure of H_2O which decreases by e.g. a factor of $\approx$10 between 298 and 265 K. The steep, decreasing vertical gradient of atmospheric H_2O also implies that the fraction of HNO_3 bound to H_2O will actually decrease to $\approx 10^{-4}$ at the tropopause [13].

5. Conclusion and atmospheric implications

The rate coefficient for the reaction of OH with HNO_3 was determined for the first time in the presence of atmospherically relevant amounts of water vapor. The rate constant obtained at 298 K showed, within experimental uncertainty, no dependence on H_2O up to 10 Torr, in a total pressure of 200 Torr N_2 and is in excellent agreement with the latest recommendations. This result rules out a significantly enhanced third body effect for H_2O compared to N_2 under our experimental conditions. As our data were obtained at a H_2O/N_2 ratio of up to 0.05, which is $\approx$ twice the maximum ratio encountered anywhere in the atmosphere, we exclude the possibility that this mechanism can enhance the $OH + HNO_3$ rate constant. Our results are also consistent with calculations that suggest that HNO_3 is not present at a significant fraction as $HNO_3 \cdot H_2O$ in our experiments, or in the atmosphere. Our measurements of the UV-absorption spectrum of HNO_3 in the presence of varying amounts of H_2O also reveal no significant difference to the spectrum of anhydrous HNO_3, and significant perturbation of the photodissociation lifetime of HNO_3 due to molecular interaction with H_2O vapor can also be excluded.

References

[1] S.S. Brown, R.K. Talukdar, A.R. Ravishankara, J. Phys. Chem. 103 (1999) 3031.
[2] M.G. Schultz, D.J. Jacob, J.D. Bradshaw, S.T. Sandholm, J.E. Dibb, R.W. Talbot, H.B. Singh, J. Geophys. Res. 105 (2000) 6669.
[3] A.N. Thakur, H.B. Singh, P. Mariani, Y. Chen, Y. Wang, D.J. Jacob, G. Brasseur, J.-F. Müller, M. Lawrence, Atmos. Environ. 33 (1999) 1403.
[4] S.P. Sander, R.R. Friedl, W.B. DeMore, D.M. Golden, M.J. Kurylo, R.F. Hampson, R.E. Huie, G.K. Moortgat, A.R. Ravishankara, C.E. Kolb, M.J. Molina, Chemical kinetics and photochemical data for use in stratospheric modelling, Supplement to evaluation 12, Updata of key reactions, Jet Propulsion Laboratory, 2000.
[5] W.B. DeMore, S.P. Sander, D.M. Golden, R.F. Hampson, M.J. Kurylo, C.J. Howard, A.R. Ravishankara, C.E. Kolb, M.J. Molina, Chemical kinetics and photochemical data for use in stratospheric modelling, No. 12, Jet Propulsion Laboratory, 1997.
[6] D. Bauer, T. Ingham, S.A. Carl, G.K. Moortgat, J.N. Crowley, J. Phys. Chem. 102 (1998) 2857.
[7] R.P. Wayne, I. Barnes, P. Biggs, J.P. Burrows, C.E. Canosa-Mas, J. Hjorth, G. Le Bras, G.K. Moortgat, D. Perner, G. Poulet, G. Restelli, H. Sidebottom, Atmos. Environ. 25A (1991) 1.
[8] S.S. Brown, J.B. Burkholder, R.K. Talukdar, A.R. Ravishankara, J. Phys. Chem. 105 (2001) 1605.
[9] A.R. Curtis, W.P. Sweetenham, Facsimile; AERE, Report R-12805, 1987.
[10] C.C. Kircher, S.P. Sander, J. Phys. Chem. 88 (1984) 2082.
[11] R.-R. Lii, M.C. Sauer, S. Gordon, J. Phys. Chem. 85 (1981) 2833.
[12] S. Aloisio, J.S. Francisco, J. Phys. Chem. 102 (1998) 1899.
[13] F.M. Tao, K. Higgins, W. Klemperer, D.D. Nelson, Geophys. Res. Lett. 23 (1996) 1797.
[14] J.B. Burkholder, R.K. Talukdar, A.R. Ravishankara, S. Solomon, J. Geophys. Res. 98 (1993) 22937.